

# Emergent properties in optically bound matter

J. M. Taylor<sup>1</sup>, L. Y. Wong<sup>2</sup>, C. D. Bain<sup>2</sup>, and G. D. Love<sup>1</sup>

<sup>1</sup> Department of Physics, Durham University, South Road, Durham DH1 3LE, UK

<sup>2</sup> Department of Chemistry, Durham University, South Road, Durham DH1 3LE, UK

[j.m.taylor@dur.ac.uk](mailto:j.m.taylor@dur.ac.uk)

**Abstract:** Sub-micron particles have been observed to spontaneously form regular two-dimensional structures in counterpropagating evanescent laser fields. We show that collective properties of large numbers of optically-trapped particles can be qualitatively different to the properties of small numbers. This is demonstrated both with a computer model and with experimental results. As the number of particles in the structure is increased, optical binding forces can be sufficiently large to overcome the optical landscape imposed by the interference fringes of the laser beams and impose a different, competing structure.

© 2008 Optical Society of America

**OCIS codes:** (290.4020) Mie theory; (170.4520) Optical confinement and manipulation; (160.4670) Optical materials; (240.6700) Surfaces

---

## References and links

1. A. Ashkin, J. M. Dziedzic, J. E. Bjorkholm, and S. Chu, "Observation of a single-beam gradient force optical trap for dielectric particles," *Opt. Lett.* **11**, 288–290 (1986).
2. M. M. Burns, J.-M. Fournier, and J. A. Golovchenko, "Optical Binding," *Phys. Rev. Lett.* **63**, 1233–1236 (1989).
3. M. M. Burns, J.-M. Fournier, and J. A. Golovchenko, "Optical Matter: Crystalization and binding in intense optical fields," *Science* **249**, 749–754 (1990).
4. N. K. Metzger, E. M. Wright, and K. Dholakia, "Theory and simulation of the Bistable behaviour of optically bound particles in the Mie size regime," *New J. Phys.* **8**, 139 (2006).
5. N. K. Metzger, K. Dholakia, and E. M. Wright, "Observation of Bistability and Hysteresis in optical binding of two dielectric spheres," *Phys. Rev. Lett.* **96**, 068102 (2006).
6. P. J. Reece, E. M. Wright, and K. Dholakia, "Experimental observation of modulation instability and Optical Spatial Soliton Arrays in soft condensed matter," *Phys. Rev. Lett.* **98**, 203902 (2007).
7. J. Ng, Z. F. Lin, C. T. Chan, and P. Sheng, "Photonic clusters formed by dielectric microspheres: numerical simulations," *Phys. Rev. B* **72**, 085130 (2005).
8. C. D. Mellor and C. D. Bain, "Array formation in evanescent waves," *ChemPhysChem* **7**, 329–332 (2006).
9. C. D. Mellor, T. A. Fennerty, and C. D. Bain, "Polarization effects in optically bound particle arrays," *Opt. Express* **14**, 10079–10088 (2006).
10. S. A. Tatarikova, A. E. Carruthers, and K. Dholakia, "One-Dimensional Optically Bound Arrays of Microscopic Particles," *Phys. Rev. Lett.* **89**, 283901 (2002).
11. D. McGloin, A. E. Carruthers, K. Dholakia, and E. M. Wright, "Optically bound microscopic particles in one dimension," *Phys. Rev. E* **69**, 021403 (2004).
12. T. Čížmár, M. Šiler, M. Šerý, P. Zemánek, V. Garcés-Chávez, and K. Dholakia, "Optical sorting and detection of submicrometer objects in a motional standing wave," *Phys. Rev. B* **74**, 035105 (2006).
13. K. Dholakia and P. Reece, "Optical micromanipulation takes hold," *Nano Today* **1**, 18–27 (2006).
14. M. Abramowitz and I. A. Stegun, *Handbook of Mathematical Functions* (Dover, 1972).
15. H. C. van de Hulst, *Light Scattering by Small Particles* (Dover, New York, 1981).
16. Y.-L. Xu, "Electromagnetic Scattering by an Aggregate of Spheres," *Appl. Opt.* **34**, 4573–4588 (1995).
17. D. W. Mackowski, "Analysis of Radiative Scattering for Multiple Sphere Configurations," *Proc. R. Soc. London, Ser. A* **433**, 599–614 (1991).
18. J. P. Barton, D. R. Alexander, and S. A. Schaub, "Theoretical determination of Net Radiation Force and Torque for a Spherical Particle Illuminated by a focused laser beam," *J. Appl. Phys.* **66**, 4594–4602 (1989).

19. M. Doi and S. F. Edwards, *The Theory of Polymer Dynamics*, International Series of Monographs on Physics (Clarendon Press, Oxford, 1986).
  20. P. E. Kloeden and E. Platen, *Numerical Solution of Stochastic Differential Equations* (Springer-Verlag, 1992).
  21. M. Šiler, M. Šery, T. Čižmár, and P. Zemánek, "Submicron particle localization using evanescent field," *Proc. SPIE* 5930, 59300R (2005).
  22. J. Ng and C. T. Chan. Private communication.
  23. J. Lekner, "Force on a scatterer in counter-propagating coherent beams," *J. Opt. A* 7, 238–248 (2005).
- 

## 1. Introduction

Optically bound matter [1, 2, 3] describes arrays of microscopic particles whose structure is controlled and affected by optical binding, or a distribution of forces formed by light. Individual Rayleigh particles are attracted to regions of higher intensity. However, a key feature in optical matter is that the positions of the particles themselves modifies the light distribution, and the light distribution in turn affects the motion of the particles, giving the potential for rich nonlinear behaviour [4, 5, 6].

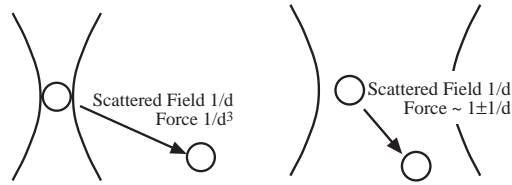
At sub-micron scales there are preferred "bond lengths" and angles between nearby particles, which lead to complicated, regular structures [7, 8, 9]. These can occur even in a uniform background field: the scattered wave from a particle interferes with the background field to produce a spatial intensity modulation. While the mechanism of longitudinal optical binding in larger particles has received attention from a number of groups [2, 10, 5, 11], lateral binding [7, 6] is less well understood. In this letter we describe the results of a simulation based on rigorous scattering theory to describe optical binding, and compare the results with experiment. This explicitly shows for the first time that the bulk behavior of many-particles is different to that of isolated particles. An unusual feature of optical binding is that the interaction strength scales with the inverse of distance,  $r$ , as observed in [7]. To our knowledge the physical reason for this has not been discussed in detail in the literature, and here we describe theoretically why this happens, and show how it leads to the observed optically bound structures. As well as being theoretically interesting, potential applications include the manipulation of biological material, the transport and sorting of trapped particles [12], and the self-assembly of complex structures [13]. As well as being important for experiments involving optically-bound clusters of particles, our findings highlight the limitations in assuming that the transport and sorting of particles can be accurately analyzed by treating individual particles in isolation.

The experimental setup we consider is described in detail in Ref. [9]. Briefly, two counter-propagating lasers are incident on a glass-water interface in a prism at an angle greater than the critical angle which creates an evanescent field which traps sub-micron dielectric particles. If the beams' polarizations are the same, interference fringes are formed and this creates a regular "optical landscape". If orthogonal polarizations are used – or if incoherent beams are used – there are no fringes, but particles are still able to form regular structures due to the effects of light multiply-scattered between the particles [9, 7].

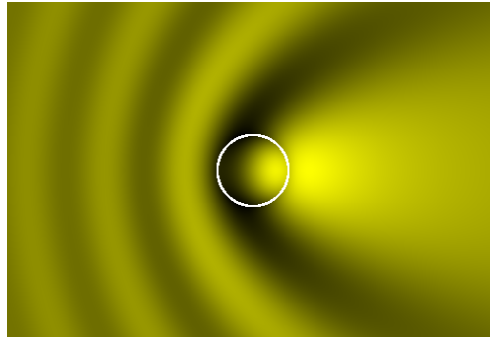
## 2. Optical binding theory

Before describing our model, we first discuss the  $1/r$  force relationship for optical binding. This relationship was derived in [3], but we present a more physically intuitive explanation here. Consider the scattered wave from a single particle. The amplitude of this wave decays as  $1/r$  and hence its intensity decays as  $1/r^2$ . The gradient force on a second particle lying outside the illuminating beam is proportional to the gradient of intensity, and will therefore be proportional to  $1/d^3$ , where  $d$  is the distance between the two particles.

If, on the other hand, a second particle is also inside the illuminating beam, the scattered light interferes with the background laser light, forming fringes. A simple example of this is



(a) Optical binding scaling



(b) Interference of scattered wave and laser field

Fig. 1. (a) Schematic showing how the scattered intensity of light from a single particle (left) in a beam depends on  $1/r$ , and therefore the gradient force on the second particle outside the beam depends on  $1/d^3$  for particle separation  $d$ . When both particles are exposed to the laser field (right), the modulation in the force scales with  $1/d$ . (b) Simulation showing the field intensity distribution caused by interference of a scattered wave from a particle with the evanescent field of a single laser beam propagating left to right, showing the production of interference fringes which lead to optical binding.

shown in Fig. 1. The fringe amplitude varies as  $1 \pm \alpha/r$  (where  $\alpha$  is a measure of the level of scattering by the particle). Thus their intensity varies as

$$(1 \pm \alpha/r)^2 \sim 1 \pm 2\alpha/r, \quad (1)$$

where we have for now made the approximation that the scattered field is a small perturbation to the laser field. Since the gradient force is proportional to intensity, we find that in addition to the effect of the external beam there is a force acting on the second particle whose strength varies as  $1/d$ . Thus even for a one-dimensional chain, the magnitude of the forces on the central particle can grow indefinitely with the length of the chain. Consider a chain of  $2n + 1$  particles with spacing  $d$  such that for a particle  $i$  at position  $id$  the scattered waves from every other particle are in phase. For large  $n$  the strength of the forces on the central particle will scale as

$$|F| \sim 1 + \sum_{i=1}^n \frac{2\alpha}{id} \sim 1 + \frac{2\alpha(\ln n + \gamma)}{d}, \quad (2)$$

where  $\gamma = 0.5772\dots$  is the Euler-Mascheroni constant [14, Eq. 6.1.3]. The force is a logarithmically-increasing function of  $n$ . This is in contrast to an electrostatic interaction which would asymptotically approach a constant value at large  $n$ .

Next we describe our computer model and present detailed simulation results. Our model uses Generalized Lorentz-Mie Theory (GLMT) [15, 16, 17, 18] to calculate the field and force

on a group of spherical particles. The field calculation is exact for spherical nonmagnetic particles; the main assumption in the numerical results presented here is that we ignore the effect of light re-scattered by the prism/air interface. This has been ignored because of the technical difficulty in treating the reflection from a planar surface in a basis of spherical waves. For convenience we also use a local plane wave approximation for the loosely-focused incident Gaussian beam. The model is applicable to spheres of any size from Rayleigh spheres all the way up to the ray optics regime, although in practice multiple-sphere calculations are limited by computer memory and numerical precision to sphere radii of around  $30\lambda$ .

The code can also simulate Brownian motion [19, 20] to check stability against thermodynamic fluctuations. It has been observed (see for example [7]) that there are many different-shaped configurations of a given number of particles that are local energy minima, but in experiments we don't observe as many variations [9]. This is because, at least in the case of silica and polystyrene particles, we find the energy required to break up most of the structures is very low, and in practice the particles will end up in one of a small number of thermally stable structures.

We do not describe the technical details of our model here as the pertinent equations are derived and listed in the references given above. Except where otherwise specified, the numerical parameters used in the calculations presented here are as listed in Table 1.

Parameter	Value	Comment
Vacuum wavelength	1064nm	Nd:YAG laser
Laser beam power	300mW	
Focal spot size	$8\mu\text{m}$	
Substrate refractive index	1.45	Silica prism
Water refractive index	1.32	Particles in water
Critical angle	$65.6^\circ$	
Angle of incidence	$67^\circ$	
Particle refractive index	1.57	Polystyrene

Table 1. Parameters used in the calculations in this paper. In addition we refer to the particle radius  $a$  and the size parameter  $ka$  where  $k$  is the laser wavenumber in water.

### 3. Fringe affinity of a chain of particles

The behaviour of a single particle in the presence of interference fringes has previously been considered by several groups [21, 22, 23] in GLMT calculations like our own. Figure 2 shows the results of our simulation and shows the force on a single particle in a set of interference fringes as a function of particle size parameter  $ka$ , where  $k$  is the wavenumber in water and  $a$  is the particle size. When the electric field of the laser is in the trapping plane, this is designated "S" polarization. Similarly "P" polarization is when the polarization is parallel to the plane of incidence. The plot shows that a single, small particle is attracted to bright fringes. At larger radii the particle's centre can instead be attracted to a dark region between fringes.

For a particle whose refractive index is close to that of the surrounding medium, this can also be understood through a gradient potential argument. For some sizes of particle, the integrated intensity within the volume of the sphere is maximized when the particle is centred on the dark fringe *between* two bright fringes [21], because two fringes are fairly well covered by the particle instead of one fringe being very well covered (see Fig. 2). We designate the radius at which the behaviour first switches from light-seeking to dark-seeking as the "crossover radius".

Next we consider the force on a particle within a chain of particles parallel to the interference fringes, as illustrated in Fig. 3. This process was repeated for various particle radii and for S and P polarization states. The results are summarized in Fig. 4, which shows the force acting

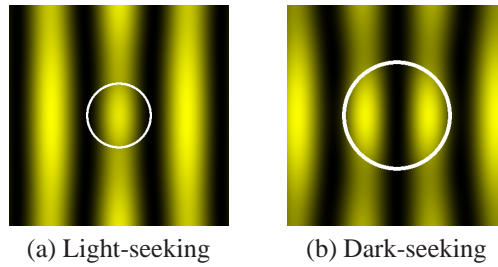
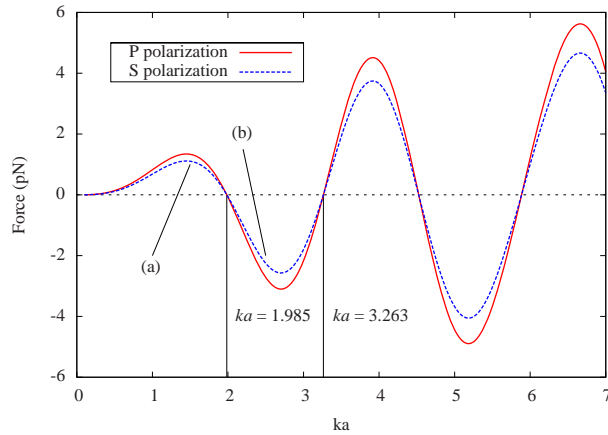


Fig. 2. The top graph shows the force acting on a single particle placed halfway between a bright and dark fringe, as a function of size parameter  $ka$ . A positive force indicates that the particle is attracted to the bright fringe. Two lines are shown for different polarization states. The first crossover occurs at  $ka = 1.985$ . For full parameters used, see Table 1. It can be seen that for a range of values of  $ka$  the force is negative and therefore particles are attracted to darker regions. The “crossover” sizes (where the particles switch from being attracted to light to dark) are indicated numerically on the graph. The lower two plots show simulated images showing how the interference fringes are distorted by the particle and that the particle sits on a bright fringe when small (a) and on a dark fringe when larger (b). The white circles indicate the particle size and location, and the size parameters for (a) and (b) are indicated on the graph.

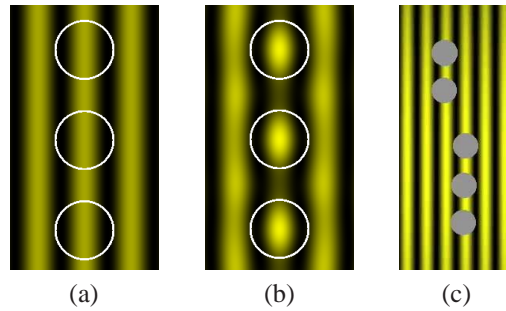


Fig. 3. Examples of chains of particles along the fringe direction. (a) is shown without scattered light, for clarity. (b) shows how the fringe pattern can be modified by the presence of the spheres. (c) Movie (1.3MB) shows a simulation demonstrating the switch in fringe affinity for 265nm radius particles as more particles are added to the system. The particles are free to move in three dimensions in this simulation (though they are of course physically constrained by the surface of the prism).

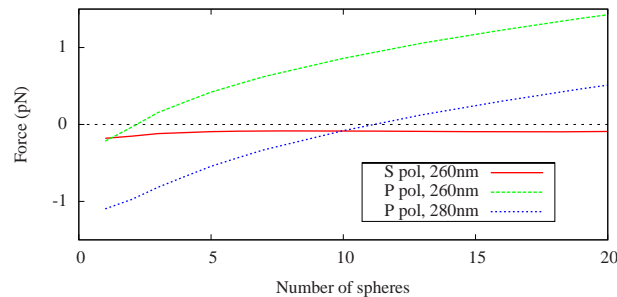


Fig. 4. Force acting on the central particle of a chain of particles as a function of number of spheres in the chain. The forces are shown for both S and P laser polarizations for spheres of radius 260nm, and for P polarization for spheres of radius 280nm. A positive force indicates that the particle is attracted to the bright fringe, and a negative force a dark fringe. For full parameters used, see Table 1.

on the central particle in a chain halfway between a fringe maximum and a fringe minimum (in analogy to Fig. 2). From this we determine whether the chain is attracted to a bright or dark fringe and the strength of that attraction.

It can be seen that in P-polarized light a large chain of particles is attracted to bright fringes despite the fact that a single particle is attracted to dark fringes. The force acting on an individual particle in the chain grows with the size of the chain. Figure 5 shows the scattering behaviour in various situations, which leads to field distributions such as that shown in Fig. 3 and explains the different behaviour for S and P-polarized light.

There is competition between the external optical landscape of the fringes, which in this case attracts an individual particle towards dark regions, and the scattering behaviour of the ensemble of particles which tends to attract the ensemble towards bright fringes. The force due to the interference fringes is smallest close to the “crossover radius”, and hence a chain of only 3 particles of radius 260nm is able to overcome the influence of the “landscape” and settle on a bright fringe. For 280nm particles, a chain of 13 particles is required to overcome the increased force of the landscape.

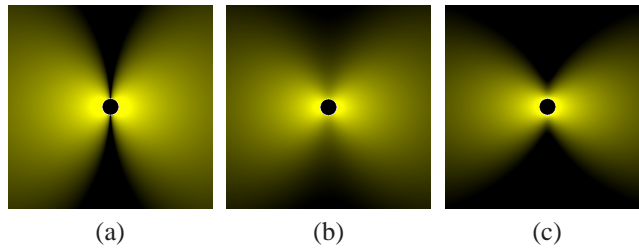


Fig. 5. Scattered field intensity in the trapping plane for a particle with  $ka = 2.5$ . The intensity is displayed on a logarithmic scale. (a) P-polarized beams and particle on a dark fringe. There is no scattering in the direction of the fringes when a particle lies on a dark fringe. (b) P-polarized beams and particle on a light fringe. A particle situated on a bright fringe formed by P-polarized light scatters relatively strongly in the direction of the fringes. This scattering enhances the intensity of the fringe that the particle lies on, which makes it more energetically favourable for other particles to be situated on that same fringe. (c) S-polarized beams and particle on a light fringe. There is very weak far-field scattering in the direction of the fringes (a dipole scatterer will not scatter in a direction parallel to the electric field polarization).

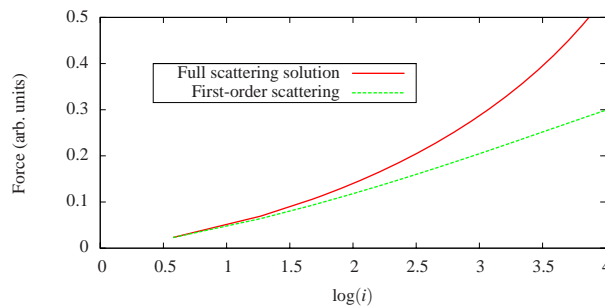


Fig. 6. Force acting on the central of  $(2i + 1)$  particles. We can compare this logarithmic plot to our Eq. 2, which predicted a logarithmic relationship. While we were correct in predicting that the force would continue to grow with the number of particles, rather than converging to a constant value, the equation has under-estimated the growth of the force. The reason for this is that the equation only used a simplistic treatment of the first-order scattered field. Also shown here is the force due only to the first-order scattered field (using the order-of-scattering method [16], we terminated the iteration at first order). The form of that curve is indeed well predicted by Eq. 2.

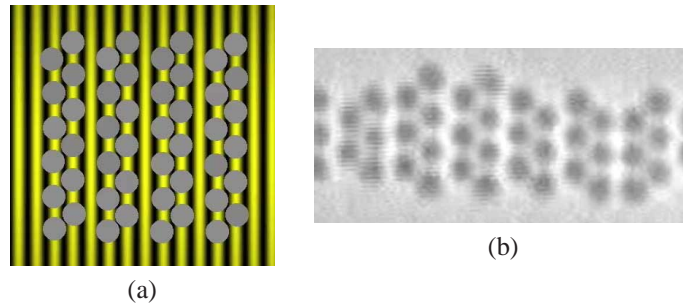


Fig. 7. Examples of “broken hex” optically-bound structures with vacant fringes. (a) shows a snapshot from a Brownian dynamics simulation, and (b) shows an experimental image. In both cases the particle radius is 260nm. In the experimental image the vertical extent of the particle array is limited by the shape of the focused Gaussian beams.

Figure 6 compares our numerical results with the prediction of Eq. 1. This supports our description of optical binding as a long-range interaction scaling with  $1/r$ , but shows that the picture is complicated by multiple scattering: optical binding has become the dominant influence on the optical landscape, and the perturbation approach taken earlier is no longer entirely appropriate. Nevertheless, the argument used to arrive at Eq. 2 is a good starting point for understanding the origins of the long-range nature of the interaction.

Finally, we extended our analysis to two-dimensional structures and included the effects of Brownian motion. Here we found that along the fringe direction, the behavior was very close to that already described for single chains. The main effect in the orthogonal direction, perpendicular to the fringes, is that there is not physically room (for the interesting case of larger particles) for a close-packed lattice with a lattice constant in the fringe direction matching that of the 1D chain. As a result a stable structure must contain vacant fringes, and the particles are slightly offset from the fringe centres. An example result from our simulation is shown in Fig. 7(a). This is extremely similar to the structures previously observed in experiments [9], shown in Fig. 7(b). The simulation has shown that structures of greater than a few tens of particles are stable against thermal fluctuations, which matches experimental observations.

#### 4. Conclusions

In conclusion, we have shown both with theory and experiments that the behaviour of a large cluster of trapped dielectric particles is qualitatively different from that of individual particles. We have justified a simple  $1/r$  relationship for optical binding, and have demonstrated its use in the limit of small perturbations. We have shown that a full Mie scattering model can be applied even where there is strong feedback through multiple scattering. We have analyzed a 1D case in detail, and shown that when extended to the 2D case our computer model agrees with experimental data.

Our findings have important implications for attempts to understand the physics of trapping experiments involving large numbers of particles. We have demonstrated the richness of behaviour exhibited by optically trapped particles, but shown that great caution must be taken if using a “ground-up” approach of considering the behaviour of a single particle (or a small number of particles) and generalizing those conclusions to larger clusters of particles.

## **Acknowledgments**

This work was funded in part by the EPSRC and the EU under the SONS-EUROCORES program (SPANAS).